applied sciences

MDPI

Article

Changes in Morphology and Bone Mineral Density of Human Mandibular Condyle During Orthodontic Treatment

Jonathan Shue [1], Ian Segall [1], Sonya Kalim [2], Jinju Kim [1], Henry W. Fields [1], J. Martin Palomo [3] and Do-Gyoon Kim [1,*]

[1] Division of Orthodontics, The Ohio State University, 4088 Postle Hall 305 W. 12th Ave, Columbus, OH 43210, USA; jishue13@gmail.com (J.S.); isegall12@gmail.com (I.S.); jinju@youngki.org (J.K.); fields.31@osu.edu (H.W.F.)
[2] Workman School of Dental Medicine, High Point University, High Point, NC 27268, USA; skalim@highpoint.edu
[3] Department of Orthodontics, School of Dental Medicine, Case Western Reserve University, Cleveland, OH 44106, USA; jmp5@case.edu
* Correspondence: kim.2508@osu.edu; Tel.: +1-(614)-247-8089; Fax: +1-(614)-688-3077

Abstract

The objective of the present study was to investigate whether orthodontic treatment alters the morphology and bone mineral density (BMD) distribution of the mandibular condyle in growing adolescent patients. Cone-beam computed tomography (CBCT) images were retrospectively analyzed for 29 patients (10 males and 19 females, aged 12.5 to 17.0 years) treated with full fixed orthodontic appliances. The right and left mandibular condyles were digitally isolated. For the internal control sample, the basal cortical bone (CB) at both mandibular first molar sites was also digitally dissected. A frequency plot of the CBCT gray values, proportional to BMD, was analyzed to calculate the mean and the 5th percentile of low and high gray values (Low_5 and $High_5$). Morphological changes in the condylar surface were assessed based on temporomandibular joint osteoarthritis (TMJOA) counts. Lateral cephalometric radiographs were used to measure facial morphology parameters and classify skeletal patterns. The cervical vertebral gray values of the same patients were compared. No radiographic signs of TMJ disorder were observed with no significant difference in TMJOA counts between before and after treatment ($p = 0.56$). The volume, mean and Low_5 gray values of the mandibular condyle, facial morphology parameters, and cervical vertebral gray values significantly increased following orthodontic treatment ($p < 0.05$). Skeletal Class II patients exhibited greater changes in mean, Low_5, and $High_5$ mandibular condyle gray values compared to their Class I patients ($p < 0.05$), whereas cervical vertebral gray values were not significantly influenced by skeletal classification ($p > 0.19$). The findings suggest that orthodontic treatment, combined with natural patient growth, contributes to nonpathological condylar alterations in adolescent patients.

Keywords: orthodontic treatment; temporomandibular joint; mandibular condyle; cone beam computed tomography; bone mineral density

Check for updates

Academic Editor: Jong-Moon Chae

Received: 3 December 2025
Revised: 30 December 2025
Accepted: 4 January 2026
Published: 7 January 2026

Copyright: © 2026 by the authors. Licensee MDPI, Basel, Switzerland. This article is an open access article distributed under the terms and conditions of the Creative Commons Attribution (CC BY) license.

1. Introduction

The mandibular condyle at the temporomandibular joint (TMJ) plays an important role in articulating functional static and dynamic masticatory loading. Local characteristics of the condyle bone can be altered by bone modeling and remodeling, which are triggered and maintained depending on the magnitude of loading [1–3]. Clinical observations indicated

that bite force changes during orthodontic treatment [4,5], suggesting that the mandibular condyle can be altered by the orthodontic treatment.

A recent study observed that cortical bone growth of the mandibular condyle is completed at 22 years of age in women and 24 years in men [6], and that its volume is continuously modified with age [7,8]. These structural changes can alter the biomechanics of articulatory loading on the mandibular condyle over time [9]. Altered articulatory loading continuously stimulates bone modeling and remodeling, resulting in mechanobiological changes in the local subchondral bone during and after the completion of mandibular growth [1,9,10]. These bone changes involve the activities of bone cells, including the resorption of existing bone by osteoclasts and the formation of new bone by osteoblasts. Since existing bone tissue is more mineralized than newly formed bone tissue, alterations in bone result in a heterogeneous distribution of bone mineral density (BMD). Consequently, BMD distribution can serve as a fingerprint of the mineralization process [1,11].

The morphology of the mandibular condyle is one of the most important factors in planning orthodontic treatment. The rapid growth of the mandibular condyle during adolescence affects the shape and position of the oral and craniofacial skeleton [2,12]. Skeletal relationships between the maxilla and mandible can be altered by changes in condylar morphology. For example, orthodontic treatment of Class II malocclusions involves remodeling the articular surfaces of the condyle to improve the position of the mandible relative to the maxilla [13]. However, the effects of orthodontic treatment on the alteration of the mandibular condyle in growing adolescents are not yet fully understood.

The objective of the present study was to investigate whether orthodontic treatment alters the morphology and BMD distribution of the mandibular condyle in growing adolescent patients. Clinical 3D cone beam computed tomography (CBCT) was utilized to longitudinally obtain images of patients' oral and craniofacial skeletons before and after orthodontic treatment.

2. Materials and Methods

This retrospective study was approved by the Institutional Review Board (IRB) at The Ohio State University (Protocol No. 2023H0174). All patients included in this study underwent comprehensive orthodontic treatment with fixed orthodontic appliances at the Department of Orthodontics, College of Dentistry, Case Western Reserve University. Cone beam computed tomography (CBCT) was utilized to scan all patients for routine diagnostic purposes before and after orthodontic treatment. The CBCT images provided a 60 cm full field of view (FOV) with voxel sizes of either 292 or 377 microns under scanning conditions of 2 mA and 120 kV using the Hitachi CB MercuRay Scanner (Hitachi Medical Systems America, Twinsburg, OH, USA) (Figure 1a,b).

Patients with craniofacial anomalies or facial asymmetries, as well as those who underwent orthognathic surgery, rapid palatal expansion, and headgear treatment were excluded from the study. As a result, the current study used CBCT images obtained from orthodontic treatments that constituted a homogeneous sample, with full fixed appliances using the first molars on both sides as anchorage units. Based on the BMD values from a preliminary study, a sample of 4 CBCT images would provide the minimum data needed for bone analysis to obtain significant results ($p < 0.05$) with 95% statistical power using a two-sample paired t-test between the pre- and post-orthodontic treatment groups [15]. The final data set included CBCT images from 29 patients (10 males aged 12.7 to 16.9 years and 19 females aged 12.5 to 17.0 years) with an average age of 14.55 $\pm$ 1.37 years at onset. At post-treatment, patients were an average age of 16.21 $\pm$ 1.36 years (males aged 14.3 to 18.9 years and females aged 14.3 to 18.9 years). Treatment duration ranged from 9 to 26 months, with an average of 19.93 $\pm$ 4.54 months.

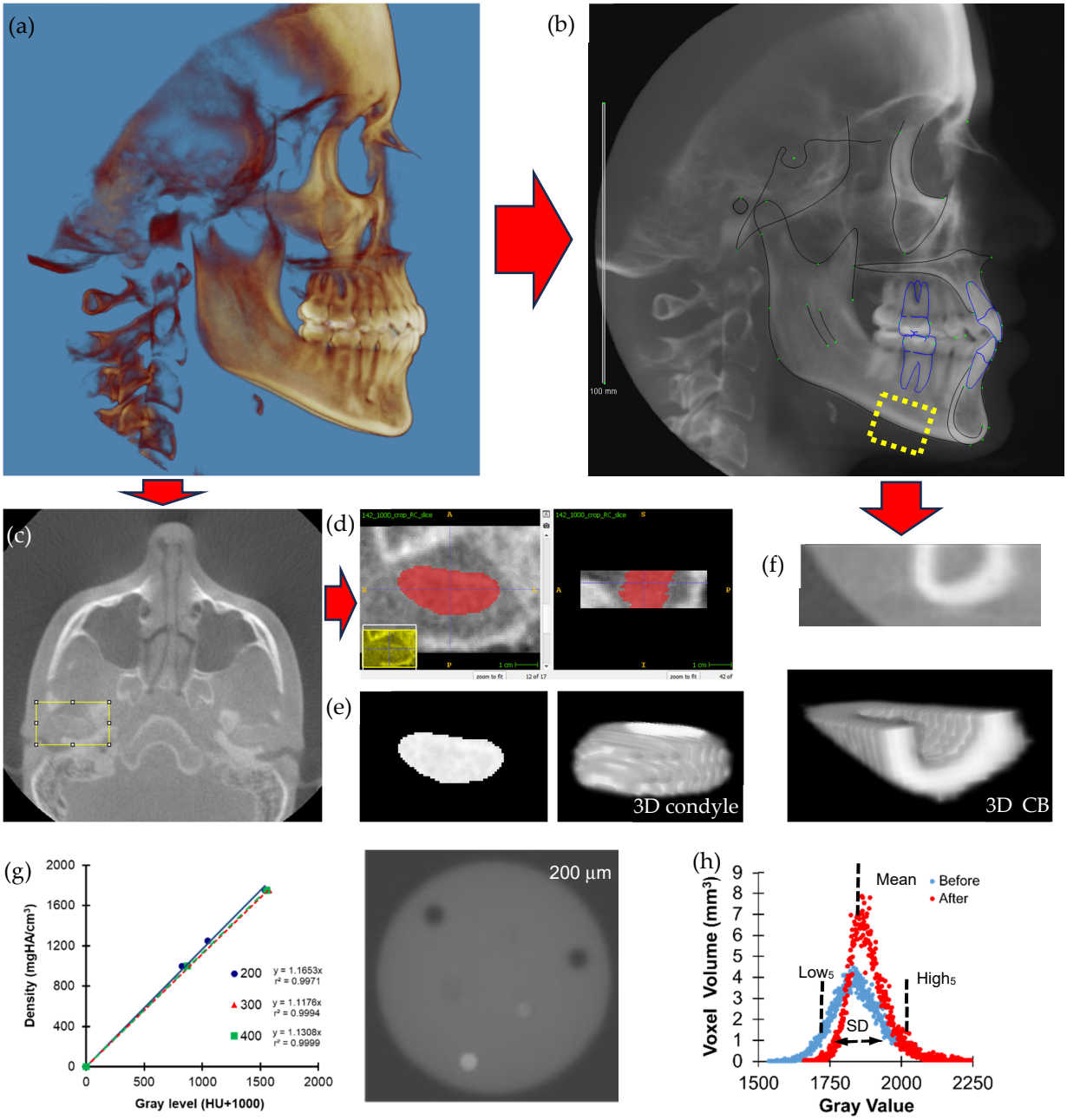


Figure 1. The process of 3D CBCT image to digitally isolate a patient's mandibular condyle (**a**) lateral view of a CBCT image in Dolphin, (**b**) lateral cephalometric radiograph extracted from CBCT image, (**c**) isolating the right condyle in ImageJ v1.47, (**d**) defining the condyle within ITK Snap, (**e**) the resulting isolated condyle which includes both trabecular and cortical bone, and (**f**) basal cortical bone (CB) at the mandibular first molar site, and (**g**) strong positive relationships between CBCT gray values obtained by 3 different scanning/reconstruction resolutions (200, 300, and 400 µm) and 3 different densities (1000, 1250, and 1750 mgHA/cm^3) of hydroxyapatite (HA) phantoms (Reprinted with unrestricted permission for non-commercial use [14]) (**h**) the gray value parameters in a frequency plot for the mandibular condyle between before and after orthodontic treatment.

The CBCT images were cropped to digitally isolate both the right and left mandibular condyles using image processing software (ImageJ, National Institutes of Health, Bethesda, MD, USA). The most superior 6.8 mm of each condyle was isolated as the condylar head (Figure 1c). ITK-SNAP software (v3.2) was used to segment the condyle from the surrounding hard and soft tissues (Figure 1d,e) following the previous study [16]. For the internal control sample, the basal cortical bone (CB) at both mandibular first molar sites

was also digitally dissected. Subsequently, the CB was isolated below the tooth root as core bone, obtained by eroding the marginal bone voxels (Figure 1f). A gray value, which is proportional to bone mineral density (BMD) was obtained using the CT attenuation values of each voxel within the condyle (Figure 1g) [14]. The mean, standard deviation (SD), and the low and high 5th percentiles (Low_5 and $High_5$) of the BMD frequency plot were calculated. This process was repeated for all 164 analyzed condyles and CBs. Cervical vertebral (CV) data were also compared to assess patients' growth. Cervical vertebral maturation (CVM) stage and cervical vertebral gray values obtained from the same patients' CBCT images were incorporated from a previous study [17].

Facial morphology was measured using a lateral cephalometric radiograph extracted from each CBCT scan with Dolphin Imaging Software (v11.95, Chatsworth, CA, USA) (Figure 1b). The following points were identified using established protocols: articulare, condylion, gonion, gnathion, lower incisor incisal edge, and lower incisor apex. The following measures were computed: mandibular length (Co-Gn) (mm); mandibular height (Ar-Go) (mm); proclination of the mandibular central incisors (L1-GoGno); and intra-mandibular divergence assessed via the gonial angle (Ar-Go-Gno). Each patient was assigned a skeletal classification based on their pre-treatment lateral cephalometric radiograph, in adherence with Anderson's statistically optimized ANB cut points [18].

TMJ osteoarthritis (OA) counts were collected according to the protocol established by a previous study [19]. Each isolated condyle was divided into three equal anteroposterior and mediolateral sections, yielding nine distinct subregions for analysis: anteromedial (AM), anterocentral (AC), anterolateral (AL), mid-medial (MM), mid-central (MC), mid-lateral (ML), postero-medial (PM), postero-central (PC), and postero-lateral (PL). A blinded examiner (S.K.) identified the presence or absence of radiographic indicators, including: flattening, loss of the rounded contour of the articular surface; erosion, loss of continuity of the articular cortical bone; osteophytes, marginal bony outgrowths of the condyle; sclerosis, increased thickness of the cortical plate in the load-bearing areas compared to the non-load bearing adjacent areas; and subchondral cyst, cavity formation below the articular surface that deviates from normal bone marrow pattern [19].

Statistical Analysis

Reliability tests for volume and gray value parameters, and cephalometric measures and TMJOA counts were conducted using the intra-Class correlation coefficient (ICC) from five randomly selected condyles. A mixed repeated measures analysis of variance (RMANOVA), with individual patients treated as a random factor, was performed to compare TMJ OA counts, volume, and gray value parameters between males and females, the left and right sides of the mandibular condyle and CB, and their interactions before and after orthodontic treatment. The same test was also used to compare morphology and gray value parameters of the cervical vertebrae (C2 and C3) before and after orthodontic treatment. Regression analyses were conducted to test associations between differences (Δ) in parameters before and after orthodontic treatment. Finally, a *t*-test was used to compare differences (Δ) in parameters before and after orthodontic treatment according to skeletal classification groupings. Statistical significance was set at $p < 0.05$.

3. Results

No change in radiographic TMJOA counts was observed using 3D CBCT images obtained before and after orthodontic treatment ($p = 0.56$). The ICCs for reliability of TMJOA counts, condylar and cervical vertebral (C2 and C3) gray values and facial morphology parameters ranged from 0.70 to 0.99. After orthodontic treatment, the volume, gray value mean and Low_5 of the mandibular condyle, gray value SD and $High_5$ of the mandibular

basal cortical bone (CB), facial morphology parameters (except for the gonial angle), and gray value mean of C2 and C3 significantly increased ($p < 0.05$) (Tables 1 and 2, and Figure 1h). In contrast, the mandibular condyle and C2 gray value SDs significantly decreased ($p < 0.04$). TMJOA counts, gray value $High_5$ of the mandibular condyle, gray value mean and Low_5 of the CB, and C3 SD did not show significant changes ($p > 0.07$) (Tables 1 and 2). Most of these results were not dependent on either sex or the side of the mandible ($p > 0.09$), except that gray value SD and $High_5$ of the CB, and mandibular length and height increased differently between males and females ($p < 0.01$).

Table 1. Comparisons of TMJ OA counts, volume, and gray value parameters for mandibular condyle and basal cortical bone (CB) between before and after orthodontic treatment for left and right sides of male and female. Significant ($p < 0.05$) differences are highlighted in **bold**.

Region		Before	After	*p* Value (Paired *t* Test)
TMJOA Counts		2.41 ± 1.23	2.48 ± 0.84	0.56
TMJ	Volume (mm^3)	743.63 ± 108.2	800.4 ± 118.97	**<0.01**
	Mean	1851.57 ± 81.24	1873.26 ± 36.3	**0.05**
	SD	74.88 ± 22.38	68.38 ± 12.78	**0.04**
	Low_5	1731.78 ± 60.42	1764.86 ± 38.66	**<0.01**
	$High_5$	1978.88 ± 113.67	1988.5 ± 47.22	0.53
CB	Mean	2514.07 ± 202.98	2504.23 ± 247.34	0.79
	SD	200.98 ± 48.72	234.59 ± 43.12	**<0.001**
	Low_5	2116.57 ± 204.93	2069.59 ± 161.11	0.09
	$High_5$	2761.19 ± 190.18	2828.17 ± 125.45	**0.01**

Table 2. Comparisons of facial morphology and gray value parameters for cervical vertebrae (C2 and C3) between before and after orthodontic treatment. Significant ($p < 0.05$) differences are highlighted in **bold**.

Region	Before	After	*p* Value (Paired *t* Test)
Md length (Co-Gn, mm)	108.17 ± 4.88	122.04 ± 5.67	**<0.01**
Md height (Ar-Go, mm)	41.77 ± 4.2	46.93 ± 5.7	**<0.01**
L1-GoGn (°)	93.53 ± 6.21	97.03 ± 7.65	**<0.01**
Ar-Go-Gn (°)	124.14 ± 5.18	123.29 ± 4.82	**<0.01**
CVM Stage	2.89 ± 1.11	3.56 ± 0.84	**<0.01**
C2 Mean	1954.68 ± 95.21	2001.57 ± 54.42	**<0.01**
C2 SD	132.57 ± 28.77	119.46 ± 12.25	**<0.01**
C3 Mean	1986.12 ± 99.4	2063.27 ± 59.26	**<0.01**
C3 SD	129.16 ± 26.96	120.32 ± 14.83	**0.01**

The changes (Δ) before and after orthodontic treatment of gray values on both sides of the mandibular condyle showed significant positive regressions with those of the CB ($p < 0.03$) except those of SD ($p > 0.12$) (Table 3). Significant but weak positive regressions were found between the changes (Δ) before and after orthodontic treatment for the mean gray value on both sides of the mandibular condyle (Δgray value mean) and the changes in the mean and SD of C2 (ΔC2 Mean and SD, $p < 0.002$) (Table 3 and Figure 2a). The Δgray

value SD on both sides of the mandibular condyle showed strong positive regressions with the Δgray value SD of C2 ($p < 0.001$) (Table 3 and Figure 2b).

Table 3. Relationship coefficients (r^2) between the changes (Δ) of the significantly different parameters before and after orthodontic treatment. Only significant ($p < 0.05$) relationships are shown in **bold**. NS: Not Significant.

Parameters		ΔC2 Gray Value Mean		ΔC2 Gray Value SD		ΔC3 Gray Value Mean		ΔC3 Gray Value SD		ΔMorphological Parameters	
		Right	**Left**	**Right**	**Left**	**Right**	**Left**	**Right**	**Left**	**Right**	**Left**
Mandibular condyle	ΔVolume (mm^3)	NS	NS	**−0.4**	**−0.17**	NS	NS	**−0.26**	**−0.16**	NS	NS
	ΔMean	**0.21**	**0.31**	**0.35**	**0.47**	NS	NS	**0.31**	**0.45**	NS	NS
	ΔSD	**0.28**	**0.25**	**0.81**	**0.81**	NS	NS	**0.87**	**0.84**	NS	NS
	ΔLow_5	NS	**0.23**	NS	**0.16**	NS	NS	NS	**0.14**	NS	NS
	$\Delta High_5$	**0.53**	**0.5**	**0.65**	**0.69**	**0.25**	**0.3**	**0.65**	**0.7**	NS	NS
CB	ΔMean	**0.37**	**0.28**	**0.43**	**0.37**	NS	NS	**0.34**	**0.34**	NS	NS
	ΔSD	NS	NS	NS	NS	NS	NS	NS	NS	NS	NS
	ΔLow_5	**0.31**	**0.37**	**0.33**	**0.38**	**0.18**	**0.19**	**0.29**	**0.39**	NS	NS
	$\Delta High_5$	**0.5**	**0.59**	**0.45**	**0.63**	**0.26**	**0.22**	**0.35**	**0.58**	NS	NS

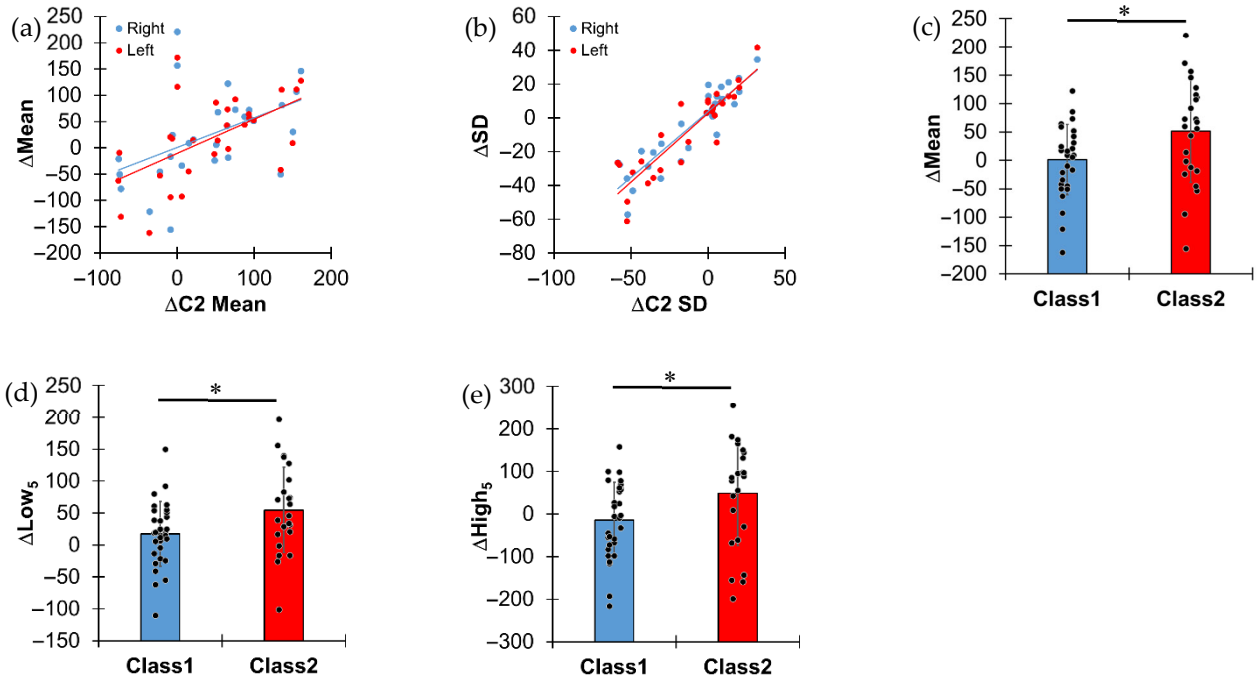


Figure 2. Significant relationships between mandibular condyle and cervical vertebra (**a**) for mean and (**b**) SD of gray value changes after orthodontic treatment (Δ). The Class II patients had more changes after orthodontic treatment for (**c**) mean, (**d**) Low_5, and (**e**) $High_5$ gray values than the Class I patients. *; $p < 0.05$.

While both pre-treatment skeletal Class I and Class II patients exhibited similar condylar and facial morphology parameter values ($p > 0.11$), orthodontic treatment resulted in significantly greater changes in the gray value mean, Low_5, and $High_5$ of the mandibular condyle, and $High_5$ of the CB in Class II malocclusion compared to Class I malocclusion ($p < 0.05$) (Table 4 and Figure 2c–e). In contrast, facial morphology and gray value parameters for cervical vertebrae did not show significant changes after orthodontic treatment across the Classes ($p > 0.19$).

Table 4. Comparison between skeletal Classification for the changes (Δ) of the significantly different parameters before and after orthodontic treatment. Significant ($p < 0.05$) differences are shown in **bold**.

Parameters		Class I (n = 15)	Class II (n = 12)	*p* Value
ΔVolume (mm^3)		58.81 ± 68.88	47.24 ± 60.44	0.52
Mandibular condyle	**ΔMean**	**1.35 ± 61.99**	**51.45 ± 89.93**	**0.03**
	ΔSD	−9.20 ± 21.59	−1.03 ± 23.33	0.19
	ΔLow_5	**17.5 ± 50.82**	**54.71 ± 66.98**	**0.03**
	$\Delta High_5$	**−14.23 ± 88.9**	**49.04 ± 123.54**	**0.04**
CB	ΔMean	−43.81 ± 191	70.2 ± 354.38	0.14
	ΔSD	26 ± 50.38	35.02 ± 51.09	0.52
	ΔLow_5	−76.4 ± 166.11	14.88 ± 245.55	0.11
	$\Delta High_5$	**14.1 ± 156.59**	**141.54 ± 222.57**	**0.02**
ΔMd length (Co-Gn, mm)		14.55 ± 3.16	13.13 ± 2.53	0.22
ΔMd height (Ar-Go, mm)		5.87 ± 3.51	4.34 ± 2.18	0.2
ΔL1-GoGn (mm)		5.24 ± 5.15	1.99 ± 8.86	0.24
ΔAr-Go-Gn (mm)		−0.29 ± 2.02	−1.22 ± 2.19	0.26
ΔC2 gray value mean		33.08 ± 69.27	58.94 ±60.42	0.32
ΔC2 gray value SD		−16.91 ± 28.52	−5.38 ± 22.35	0.26
ΔC3 gray value mean		68.43 ± 69.94	83.42 ± 57.2	0.55
ΔC3 gray value SD		−12.04 ± 24.45	−3.07 ± 20.44	0.32

4. Discussion

Bone mineral density (BMD) has been widely used to diagnose bone loss caused by osteoporosis [8,20–22]. The X-ray-based computed tomography (CT) attenuation value has been utilized to assess bone mineral density (BMD) [23]. Many animal studies have successfully described changes in tissue mineral density distribution resulting from estrogen deficiency-induced osteoporosis using high-resolution micro-CT [24–26]. Similarly, clinical studies have demonstrated that gray values (CT attenuation values) in cone-beam CT can be proportionally converted to BMD values (Figure 1f) [14,27]. As a result, heterogeneous distribution of BMD has been observed in the oral, craniofacial, and orthopedic skeleton of patients [13,14,27,28]. The current study utilized established CBCT-based morphology and BMD analysis to assess changes in the mandibular condyle of patients following orthodontic treatment.

Cervical vertebral (CV) data were compared because the CV are far enough removed from the stomatognathic system as to not be directly influenced by orthodontic forces, but previous studies indicated the close relationship of CV and condylar growth and maturation [29,30]. Increases in facial morphology, CVM stage, and mean gray value of cervical vertebrae indicate craniofacial and orthopedic bone growth and maturation during orthodontic treatment in adolescent patients, as observed in previous studies [13,31–33]. There was no increase in radiographic TMJOA indicators, lending further evidence to refute orthodontic treatment as an etiologic factor in the development of temporomandibular dysfunction [34–36]. The current study also found that the volume and BMD of the mandibular condyle significantly increased after orthodontic treatment, consistent with prior clinical observations of mandibular condylar growth in adolescent patients [2,37]. The addition of new bone results in increased condyle volume. We observed that the Low_5

gray value, which reflects the BMD of newly formed bone tissue, increased following orthodontic treatment, whereas the $High_5$ gray value, representing the BMD of pre-existing bone tissue, remained unchanged. Consequently, the mean BMD increased, while the heterogeneity (SD) of gray value distribution in the condyle decreased. This pattern was similar to changes (Δ) in the SD of gray value in C2 and C3 showing their strong positive regressions with those in mandibular condyle (Table 3 and Figure 2a,b). These findings likely reflect the rapid skeletal growth and mineralization that occur during the maturation process in adolescence [38].

However, the changes (Δ) in mean gray value in C2 and C3 could not fully explain those observed in the mandibular condyle during orthodontic treatment ($r^2 < 0.31$ or not significant, Table 3). On the other hand, the skeletal Class II group showed significantly greater changes in the mean, Low_5, and $High_5$ values of the mandibular condyle compared to the Class I group (Table 4). These results indicate that orthodontic treatment for malocclusion affects bone modeling and remodeling, altering BMD distribution in the mandibular condyle. The TMJ bears compressive loads applied by jaw muscles and articulates static and dynamic biting forces [39–41]. It has been suggested that unloading of the mandibular condyle promotes its growth, based on clinical and animal studies [1,42]. Recent clinical measurements showed that Class II patients had significantly lower bite forces than Class I patients [43]. Furthermore, bite force decreases during orthodontic treatment [6,7]. Condylar head growth has also been observed in growing skeletal Class II patients following orthodontic treatment [44]. Taken together, these findings suggest that orthodontic treatment contributes to the changes in volume and BMD in the mandibular condyle observed in the current study.

A limitation of the current study was that we could not compare potential changes in the mandibular condyle without orthodontic treatment during the same adolescent growth period. CBCT scans are limited in young individuals without oral complications due to concerns about radiation exposure. As an alternative, we included gray value analysis of the mandibular basal cortical bone (CB) as an internal control within the same patient, as this region is not directly influenced by tooth movement. As a result, we found that the $High_5$ and SD gray values in the CB significantly increased after orthodontic treatment, indicating increased mineralization of the existing bone in the CB. These findings differ from the increases in Mean and Low_5 values and the decrease in SD, which are attributable to active bone modeling and remodeling in the mandibular condyle. Furthermore, the changes (Δ) in $High_5$ values in the CB showed trends similar to those in the mandibular condyle, with significant relationships with C2 and C3, and an increase in Class II after orthodontic treatment. These findings suggest that progression of mineralization occurs during orthodontic treatment as part of the natural growth process in adolescent patients. In addition, the altered mineral distribution observed in the mandibular condyle likely reflects, at least in part, the effects of orthodontic treatment.

An additional limitation is that we did not investigate potential parameters that may influence condylar features, including a wide range of ages, genetic factors, and dentofacial phenotypes. Future studies are planned to examine the effects of these factors on the mandibular condyle.

In conclusion, the current study successfully analyzed the morphology and BMD distribution of the mandibular condyle using 3D CBCT images obtained before and after orthodontic treatment in adolescent patients. Orthodontic treatment increased the volume and BMD of the mandibular condyle without evidence of radiographic disorders in the mandibular condyle of these patients. These alterations likely result from a combination of oral and craniofacial growth and orthodontic treatment. Skeletal Class II patients showed

greater changes than Class I patients. The findings of this study provide initial information that could stimulate similar analysis in non-treated individuals.

Author Contributions: Conceptualization, J.S., I.S. and D.-G.K.; Methodology, J.S., I.S., S.K., J.K. and D.-G.K.; Software, J.S., I.S., S.K., J.K. and D.-G.K.; Validation, J.S., I.S., S.K., J.K., H.W.F., J.M.P. and D.-G.K.; Formal analysis, J.S., I.S. and D.-G.K.; Investigation, J.S., I.S., S.K., J.K., H.W.F., J.M.P. and D.-G.K.; Resources, J.M.P. and D.-G.K.; Data curation, J.S., I.S., S.K., J.K. and D.-G.K.; Writing—original draft, J.S., I.S., S.K., J.K., H.W.F., J.M.P. and D.-G.K.; Writing—review and editing, J.S., I.S., S.K., J.K., H.W.F., J.M.P. and D.-G.K.; Visualization, J.S., I.S., J.K. and D.-G.K.; Supervision, J.S., H.W.F. and D.-G.K.; Project administration, J.M.P. and D.-G.K.; Funding acquisition, D.-G.K. All authors have read and agreed to the published version of the manuscript.

Funding: The project described here was partly funded by Dr. Rudy Melfi fellowship from the College of Dentistry, The Ohio State University.

Institutional Review Board Statement: The study was conducted in accordance with the Declaration of Helsinki, and approved by the Institutional Review Board of The Ohio State University (protocol code 2023H0174).

Informed Consent Statement: Not applicable.

Data Availability Statement: The datasets presented in this article are not readily available because the data are part of an ongoing study. Requests to access the datasets should be directed to the corresponding author.

Conflicts of Interest: The authors declare no conflicts of interest.

References

1. Kim, D.G.; Jeong, Y.H.; Kosel, E.; Agnew, A.M.; McComb, D.W.; Bodnyk, K.; Hart, R.T.; Kim, M.K.; Han, S.Y.; Johnston, W.M. Regional variation of bone tissue properties at the human mandibular condyle. *Bone* **2015**, *77*, 98–106. [CrossRef] [PubMed]
2. Von den Hoff, J.W.; Delatte, M. Interplay of mechanical loading and growth factors in the mandibular condyle. *Arch. Oral Biol.* **2008**, *53*, 709–715. [CrossRef] [PubMed]
3. Smith, D.M.; McLachlan, K.R.; McCall, W.D., Jr. A numerical model of temporomandibular joint loading. *J. Dent. Res.* **1986**, *65*, 1046–1052. [CrossRef] [PubMed]
4. Therkildsen, N.M.; Sonnesen, L. Bite Force, Occlusal Contact and Pain in Orthodontic Patients during Fixed-Appliance Treatment. *Dent. J.* **2022**, *10*, 14. [CrossRef]
5. Prema, A.; Vimala, G.; Rao, U.; Shameer, A.; Gayathri. Occlusal bite force changes during fixed orthodontic treatment in patients with different vertical facial morphology. *Saudi Dent. J.* **2019**, *31*, 355–359. [CrossRef]
6. Seo, Y.S.; Park, H.J.; Yu, S.K.; Jeong, S.R.; Ryu, J.W. Evaluation of cortical bone formation on mandibular condyle in asymptomatic adolescents and young adults using cone-beam computed tomography. *Life* **2022**, *12*, 2032. [CrossRef]
7. Dudde, F.; Giese, M.; Schuck, O.; Duda, S.; Krueger, C. Panoramic radiographic analysis of age- and sex-related variations in upper mandibular morphology: Focus on the condyle, sigmoid notch, and coronoid process. *In Vivo* **2025**, *39*, 311–317. [CrossRef]
8. Shetty, S.R.; Al-Bayatti, S.; AlKawas, S.; Talaat, W.; Narasimhan, S.; Gaballah, K.; Al-Rawi, N.; Alsaegh, M.; Madiyal, A.; Balan, P.; et al. Analysis of the volumetric asymmetry of the mandibular condyles using cbct. *Int. Dent. J.* **2022**, *72*, 797–804. [CrossRef]
9. Desai, R.J.; Iwasaki, L.R.; Kim, S.M.; Liu, H.; Liu, Y.; Nickel, J.C. A theoretical analysis of longitudinal temporomandibular joint compressive stresses and mandibular growth. *Angle Orthod.* **2022**, *92*, 11–17. [CrossRef]
10. Honda, T.; Fukunaga, T.; Ito, A.; Yoshida, M.; Yasuno, K.; Tsumaki, H.; Yamaguchi, K.; Choi, Y.S.; Mizoguchi, I. Effects of mechanical load on mandibular condylar cartilage and subchondral bone of male rats. *Arch. Oral Biol.* **2025**, *177*, 106341. [CrossRef]
11. Ruffoni, D.; Fratzl, P.; Roschger, P.; Klaushofer, K.; Weinkamer, R. The bone mineralization density distribution as a fingerprint of the mineralization process. *Bone* **2007**, *40*, 1308–1319. [CrossRef]
12. Buschang, P.H.; Santos-Pinto, A.; Demirjian, A. Incremental growth charts for condylar growth between 6 and 16 years of age. *Eur. J. Orthod.* **1999**, *21*, 167–173. [CrossRef] [PubMed]
13. Shi, Q.; Gu, Z.; Lai, D.; Dai, Q.; Yu, F. Three-dimensional evaluation of condylar morphology after orthodontic treatment in adult patients with Class II malocclusion by cone-beam computed tomography. *BMC Oral Health* **2024**, *24*, 48. [CrossRef]
14. Kim, D.G. Can dental cone beam computed tomography assess bone mineral density? *J. Bone Metab.* **2014**, *21*, 117–126. [CrossRef] [PubMed]

15. Huang, H.; Richards, M.; Bedair, T.; Fields, H.W.; Palomo, J.M.; Johnston, W.M.; Kim, D.G. Effects of orthodontic treatment on human alveolar bone density distribution. *Clin. Oral Investig.* **2013**, *17*, 2033–2040. [CrossRef] [PubMed]
16. Kim, P.J.; Skabelund, Z.; Kalim, S.; Lee, C.H.; Kim, N.; Nguyen, K.; Emam, H.; Knobloch, L.; Deguchi, T.; Kim, M.; et al. Sex dependent differences of temporomandibular condylar bone mineral density distribution. *Cranio* **2025**, *43*, 321–327. [CrossRef]
17. Crawford, B.; Kim, D.G.; Moon, E.S.; Johnson, E.; Fields, H.W.; Palomo, J.M.; Johnston, W.M. Cervical vertebral bone mineral density changes in adolescents during orthodontic treatment. *Am. J. Orthod. Dentofac. Orthop.* **2014**, *146*, 183–189. [CrossRef]
18. Anderson, G.; Fields, H.W.; Beck, M.; Chacon, G.; Vig, K.W. Development of cephalometric norms using a unified facial and dental approach. *Angle Orthod.* **2006**, *76*, 612–618. [CrossRef]
19. Song, H.; Lee, J.Y.; Huh, K.-H.; Park, J.W. Long-term Changes of Temporomandibular Joint Osteoarthritis on Computed Tomography. *Sci. Rep.* **2020**, *10*, 6731. [CrossRef]
20. Seeman, E. Pathogenesis of osteoporosis. *J. Appl. Physiol.* **2003**, *95*, 2142–2151. [CrossRef]
21. Eastell, R.; O'Neill, T.W.; Hofbauer, L.C.; Langdahl, B.; Reid, I.R.; Gold, D.T.; Cummings, S.R. Postmenopausal osteoporosis. *Nat. Rev. Dis. Primers* **2016**, *2*, 16069. [CrossRef]
22. Roschger, P.; Paschalis, E.P.; Fratzl, P.; Klaushofer, K. Bone mineralization density distribution in health and disease. *Bone* **2008**, *42*, 456–466. [CrossRef] [PubMed]
23. Genant, H.; Engelke, K.; Fuerst, T.; Glüer, C.C.; Grampp, S.; Harris, S.T.; Jergas, M.; Lang, T.; Lu, Y.; Majumdar, S.; et al. Noninvasive assessment of bone mineral and structure: State of the Art. *J. Bone Miner. Res.* **1996**, *11*, 707–730. [CrossRef]
24. Kim, D.G.; Navalgund, A.R.; Tee, B.C.; Noble, G.J.; Hart, R.T.; Lee, H.R. Increased variability of bone tissue mineral density resulting from estrogen deficiency influences creep behavior in a rat vertebral body. *Bone* **2012**, *51*, 868–875. [CrossRef]
25. Liu, J.; Watanabe, K.; Dabdoub, S.M.; Lee, B.S.; Kim, D.G. Site-specific characteristics of bone and progenitor cells in control and ovariectomized rats. *Bone* **2022**, *163*, 116501. [CrossRef]
26. Kim, D.G.; Shertok, D.; Ching Tee, B.; Yeni, Y.N. Variability of tissue mineral density can determine physiological creep of human vertebral cancellous bone. *J. Biomech.* **2011**, *44*, 1660–1665. [CrossRef]
27. England, G.M.; Moon, E.-S.; Roth, J.; Deguchi, T.; Firestone, A.R.; Beck, F.M.; Kim, D.G. Conditions and calibration to obtain comparable grey values between different clinical cone beam computed tomography scanners. *Dentomaxillofac. Radiol.* **2017**, *46*, 20160322. [CrossRef] [PubMed]
28. Taylor, T.; Gans, S.; Jones, E.; Firestone, A.R.; Johnston, W.M.; Kim, D.G. Comparison of micro-CT and cone beam CT-based assessments for relative difference of grey level distribution in a human mandible. *Dentomaxillofac. Radiol.* **2013**, *42*, 25117764. [CrossRef]
29. Franchi, L.; Baccetti, T.; McNamara, J.A., Jr. Mandibular growth as related to cervical vertebral maturation and body height. *Am. J. Orthod. Dentofac. Orthop.* **2000**, *118*, 335–340. [CrossRef] [PubMed]
30. Cericato, G.O.; Bittencourt, M.A.; Paranhos, L.R. Validity of the assessment method of skeletal maturation by cervical vertebrae: A systematic review and meta-analysis. *Dentomaxillofac. Radiol.* **2015**, *44*, 20140270. [CrossRef]
31. Altan, M.; Nebioglu Dalci, O.; Iseri, H. Growth of the cervical vertebrae in girls from 8 to 17 years. A longitudinal study. *Eur. J. Orthod.* **2012**, *34*, 327–334. [CrossRef]
32. McNamara, J.A., Jr.; Franchi, L. The cervical vertebral maturation method: A user's guide. *Angle Orthod.* **2018**, *88*, 133–143. [CrossRef] [PubMed]
33. Stăncioiu, A.-A.; Vasica, F.; Nagib, R.; Popa, A.; Motofelea, A.C.; Huşanu, A.A.; Szuhanek, C.A. Cephalometric Evaluation of Facial Height Ratios and Growth Patterns: A Retrospective Cohort Study. *Appl. Sci.* **2024**, *14*, 10168. [CrossRef]
34. Luther, F. TMD and occlusion part I. Damned if we do? Occlusion: The interface of dentistry and orthodontics. *Br. Dent. J.* **2007**, *202*, E2. [CrossRef]
35. Luther, F. TMD and occlusion part II. Damned if we don't? Functional occlusal problems: TMD epidemiology in a wider context. *Br. Dent. J.* **2007**, *202*, E3. [CrossRef] [PubMed]
36. McNamara, J.A., Jr. Orthodontic treatment and temporomandibular disorders. *Oral Surg. Oral Med. Oral Pathol. Oral Radiol. Endod.* **1997**, *83*, 107–117. [CrossRef]
37. Rustia, S.; Lam, J.; Tahir, P.; Al Kharafi, L.; Oberoi, S.; Ganguly, R. Three-dimensional morphologic changes in the temporomandibular joint in asymptomatic patients who undergo orthodontic treatment: A systematic review. *Oral Surg. Oral Med. Oral Pathol. Oral Radiol.* **2022**, *134*, 397–406. [CrossRef]
38. Weaver, C.M. Adolescence. *Endocrine* **2002**, *17*, 43–48. [CrossRef]
39. Nickel, J.; Spilker, R.; Iwasaki, L.; Gonzalez, Y.; McCall, W.D.; Ohrbach, R.; Beatty, M.W.; Marx, D. Static and dynamic mechanics of the temporomandibular joint: Plowing forces, joint load and tissue stress. *Orthod. Craniofacial Res.* **2009**, *12*, 159–167. [CrossRef]
40. Herring, S.W.; Liu, Z.-J.; Rafferty, K.L.; Baldwin, M.C.; Salamati, A.; Cunningham, C.; Owart, B.; Tamasas, B. Repeated botulinum treatment of rabbit masseter causes cumulative tissue damage. *Arch. Oral Biol.* **2022**, *141*, 105480. [CrossRef]
41. Nickel, J.C.; Iwasaki, L.R.; Walker, R.D.; McLachlan, K.R.; McCall, W.D. Human Masticatory Muscle Forces during Static Biting. *J. Dent. Res.* **2003**, *82*, 212–217. [CrossRef]

42. Tuominen, M.; Kantomaa, T.; Pirttiniemi, P. Effect of altered loading on condylar growth in the rat. *Acta Odontol. Scand.* **1994**, *52*, 129–134. [CrossRef] [PubMed]
43. Ciavarella, D.; Lorusso, M.; Fanelli, C.; Ferrara, D.; Laurenziello, M.; Montaruli, G.; Esposito, R.; Tepedino, M. Evaluation of occlusal force in Class II subdivision malocclusion. *J. Oral Rehabil.* **2024**, *51*, 1813–1820. [CrossRef] [PubMed]
44. Nindra, J.; Sidhu, M.S.; Kochhar, A.S.; Dabas, A.; Valletta, R.; Rongo, R.; Spagnuolo, G. Three-Dimensional Evaluation of Condyle-Glenoid Fossa Complex Following Treatment with Herbst Appliance. *J. Clin. Med.* **2021**, *10*, 4730. [CrossRef] [PubMed]

Disclaimer/Publisher's Note: The statements, opinions and data contained in all publications are solely those of the individual author(s) and contributor(s) and not of MDPI and/or the editor(s). MDPI and/or the editor(s) disclaim responsibility for any injury to people or property resulting from any ideas, methods, instructions or products referred to in the content.